

## Image-Force Barrier Lowering of Contact Resistance for Two-Dimensional Materials: Direct Determination and Method of Images on a Cone Manifold

Sarah R. Evans,<sup>1</sup> Emeric Deylgat,<sup>1,2,3</sup> Edward Chen,<sup>4</sup> and William G. Vandenberghe<sup>1</sup>

<sup>1</sup>Department of Materials Science and Engineering, The University of Texas at Dallas.

<sup>2</sup>Department Physics, KU Leuven,

<sup>3</sup>Imec, Kapeldreef 75, 3001 Heverlee, Belgium,

<sup>4</sup>Corporate Research, Taiwan Semiconductor Manufacturing Company Ltd., Taiwan.

**Introduction:** Two-dimensional (2D) semiconducting materials have received an enormous amount of attention in the last couple of decades. [1] However, high contact resistance experienced by 2D material contacts severely inhibit practical device applications. Thus, finding methods to lower contact resistance is imperative to several 2D applications such as improving nanotube performance,[2] connecting high-mobility graphene structures through metallic contacts,[3] and improving electrical contacts.[4] Recently, we found that the permittivity of the surrounding material can enhance the Schottky barrier lowering up to 50 times.[5] Despite the importance of IFBL to the contact resistance of devices at the nanoscale, it is often ignored when analyzing the Schottky barrier height. However, the reason for neglecting IFBL is because to date, there exists no way to model the majority of contact geometries with the method of images, which requires specific geometric symmetry about the metal and the electron.

In this abstract, we present a general solution for determining the IFBL energy which can be applied to an electron near a geometry of metal with surfaces separated by an angle  $\Omega$ . First, we solve Poisson's equation using the appropriate boundary conditions and then we prove that our solution can be obtained using the method of images, provided a cone-manifold space is used.

**Methods:** Figure 1 demonstrates the geometry of a 2D top-contact, which is experimentally the most prevalent approach. It is an example of a contact geometry for which there exists no known expression of IFBL because the method of images cannot be used. The coordinate system used in the derivation is also shown.

We determine IFBL energy by solving Eq. (1) in Figure 6 as a function of position with  $(r, \theta, z)$  in addition to the location of the exciting electron,  $(r_0, \theta_0, z_0)$ . We are only interested in the obtaining  $V_1$ , or the potential resulting from the charge induced on the metal by the nearby electron. Thus, we will take the potential of the entire system,  $V$ , and subtract out the Coulomb potential of the electron,  $V_C$ , to obtain  $V_1$ , as seen in Figure 2. We assume a solution of the form  $V(r, \theta, z) = R(r)\Theta(\theta)Z(z)$  and solve Poisson's equation using the Kontorovich-Lebedev transform.[6] Equations (2) and (3) demonstrate the resulting solutions for  $\Theta(\theta)$ , (2) using the boundary conditions for a point charge in free space and (3) for a point charge in near a metal wedge. After subtracting  $V_C$  from  $V$ , the contributions of the metal are

isolated and the resulting  $V_1$  is depicted in Eq. (4). Finally, we set  $r = r_0$ ,  $\theta = \theta_0$  and  $z = z_0$ , and the final equation for image potential energy is determined as Eq. (5).

Next, we expand method of images over a non-Euclidean space to prove that we can obtain the same result. We consider a cone manifold space where we 'unfold' our metal such that it always appears flat to the electron and an image charge can now easily be placed, as illustrated in Figure 4. Solving again for  $\Theta(\theta)$ , this time with boundary conditions that consider the cone manifold space, we obtain Eq. (6). The method of images now immediately yields the potential for the system by adding the same potential of the charge with an opposite sign on the other side of the metal plate. The resulting IFBL energy is shown in Eq. (7) and can be proven equal to Eq. (5) through trigonometric identities.

**Results:** Figure 3 plots the IFBL with  $\Omega = 3\pi/2$  and  $\epsilon = 3.9\epsilon_0$ , which is the permittivity of  $\text{SiO}_2$ . We find that far from the corner, the IFBL of a bulk contact is recovered and that the IFBL weakens as the corner is approached. From visual inspection, we see that the Schottky barrier can be lowered by more than 0.1eV due to IFBL, which could improve contact resistance by orders of magnitude. In Figure 5, we consider several different contact geometries and show by how much the IFBL scales compared to a bulk contact. We find that the IFBL can be increased by a factor of 2.69 relative to a bulk contact provided an optimal geometry is used.

**Conclusion:** In summary, we determined a general solution for the IFBL emerging from two metals separated by an angle  $\Omega$  and expand the method of images using a cone manifold space. We show that IFBL can provide significant improvement to contact resistance and demonstrate how fabricating contacts to 2D materials with an optimized contact angle should significantly reduce the contact resistance. Additionally, because IFBL is scaled by permittivity, our results highlight the importance of choosing a low-permittivity dielectric surrounding the 2D material.

**Acknowledgements:** This material is based upon work supported by the Taiwan Semiconductor Manufacturing Company, Ltd.

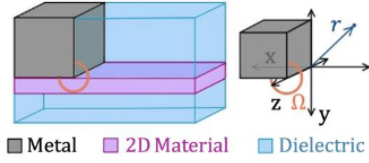


Figure 1: Illustration of a metal making a side contact to a 2D semiconductor and the coordinate system used in our derivation

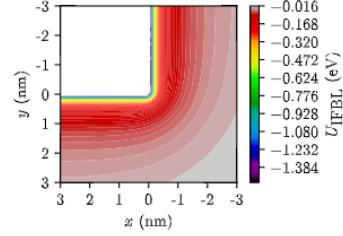


Figure 3: Plot of IFBL energy of an electron as a function of x and y with  $\Omega = 3\pi/2$  and  $\epsilon = 3.9\epsilon_0$ , which is the permittivity of  $\text{SiO}_2$

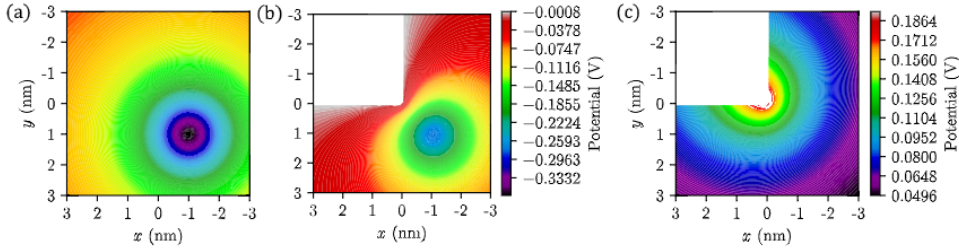


Figure 2: Graphs taken at  $z = 0$  of (a)  $V_C$ , the potential caused by a single electron located at  $(r_0, \theta_0, z_0) = (\sqrt{2}, 3\pi/4, 1)$ , b)  $V$ , the potential an electron experiences in the presence of a metal wedge with  $\Omega = 3\pi/2$ , and c)  $V_I$ , the attractive potential exerted by the metal wedge due to the presence of the electron. Note that  $V_I = V - V_C$ .

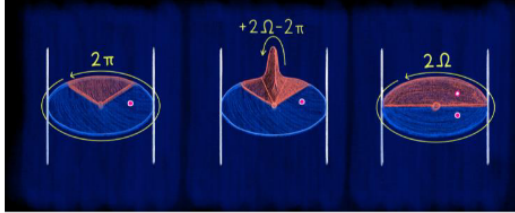


Figure 4: Illustration on how expanding Euclidean space with an additional  $2\Omega - 2\pi$  in the metal region yields a cone manifold (right) where the method of images can be used. An electron is represented with a pink dot; its image with a white dot.

	$\Omega$	$\theta$	$U_{IFBL}/(-e^2/(16\pi\epsilon r))$
a	$\pi$	$\pi/2$	1
b	$\pi$	$\pi$	$\csc(\theta)$
c	$2\pi$	$\pi$	$2/\pi \approx 0.63$
d	$3\pi/2$	$\pi$ ( $\alpha\pi/\pi/2$ )	$6 - 2/\sqrt{3} \approx 0.85$
e	$4\pi/3$	$\pi$	$8\sqrt{3}/9 + 1/\pi - 3/4 \approx 2.21$
f	$2\pi$	$3\pi/2$	$1/\pi + 1/2 \approx 0.82$
g	$3\pi/2$	$\Omega/2 = 3\pi/4$	$2 + 2\sqrt{2} - 16\sqrt{3}/9 \approx 0.74$
h	$4\pi/3$	$\Omega/2 = 2\pi/3$	$4/\sqrt{3} - 3/2 \approx 0.81$
i	$2\pi/3$	$\Omega/2 = \pi/3$	$4\sqrt{3}/9 + 2/\pi \approx 1.41$
j	$\pi/2$	$\Omega/2 = \pi/4$	$2\sqrt{2} - 1 \approx 1.8$
k	$\pi/3$	$\Omega/2 = \pi/6$	$5 - 4\sqrt{3} \approx 2.69$

Figure 5: Table showing various  $\Omega$  and  $\theta$  combinations, where  $\Omega$  indicates the shape of the metal and  $\theta$  is the angle of the semiconductor. We evaluate the resulting IFBL energy compared to bulk contact IFBL (a).

$$U_{IFBL}(r, \theta) = - \int_0^\infty \frac{q}{\epsilon} V_I(r_0, \theta_0, z_0; r, \theta, z) dq = - \frac{1}{2} e V_I \quad (1) \quad V_I = \frac{e}{4\pi\epsilon\sqrt{r r_0}} \int_0^\infty d\alpha P_{\alpha-1/2} \left( \frac{(z-z_0)^2 + r_0^2 + r^2}{2rr_0} \right) \quad (4)$$

$$\Theta_{I,\alpha}(\theta; \theta_0) = \frac{\sinh(\alpha\theta) \cosh(\alpha(\pi - (\Omega - \theta_0)))}{\alpha \sinh(\alpha\pi) \sinh(\alpha\Omega)} \quad (2) \quad \left( \frac{\sinh(\alpha\theta) \cosh(\alpha(\pi - (\Omega - \theta_0)))}{\sinh(\alpha\Omega) \cosh(\alpha\pi)} + \frac{\sinh(\alpha(\Omega - \theta)) \cosh(\alpha(\pi - \theta_0))}{\sinh(\alpha\Omega) \cosh(\alpha\pi)} \right)$$

$$\Theta_{C,\alpha}(\theta; \theta_0) = - \frac{\cosh(\alpha(\pi - |\theta - \theta_0|))}{\alpha \sinh(\alpha\pi)} \quad (3) \quad \Theta_{C,\alpha}^\ominus(\theta; \theta_0) = - \frac{\cosh(\alpha(\Omega - |\theta - \theta_0|))}{\alpha \sinh(\alpha\Omega)} \quad (6)$$

$$U_{IFBL}(r, \theta) = \frac{-e^2}{8\pi\epsilon r} \int_0^\infty d\alpha \left( \frac{\sinh(\alpha\theta) \cosh(\alpha(\pi - (\Omega - \theta)))}{\sinh(\alpha\Omega) \cosh(\alpha\pi)} + \frac{\sinh(\alpha(\Omega - \theta)) \cosh(\alpha(\pi - \theta))}{\sinh(\alpha\Omega) \cosh(\alpha\pi)} \right) \quad (5)$$

$$U_{IFBL}(r, \theta) = \frac{-e^2}{8\pi\epsilon r} \int_0^\infty d\alpha \frac{\cosh(\alpha(\Omega - 2\theta)) \sinh(\alpha\pi) + \sinh(\alpha(\Omega - \pi))}{\sinh(\alpha\Omega) \cosh(\alpha\pi)} \quad (7)$$

Figure 6: Equations used in the derivation

## References:

- [1] G. Fiori, *et al.*, "Electronics based on two-dimensional materials," *Nature nanotechnology*, 2014
- [2] R. Hafizi, *et al.*, "Band structure and contact resistance of carbon nanotubes deformed by a metal contact," *Phys. Rev. Lett.*, 2017
- [3] T. Cusati, *et al.*, "Electrical properties of graphene-metal contacts," *Scientific Reports*, 2017
- [4] A. Allain, *et al.*, "Electrical contacts to two-dimensional semiconductors," *Nature materials*, 2015
- [5] M. Brahma, *et al.*, "Contacts to two-dimensional materials: Image forces, dielectric environment, and back-gate," in *VLSI-TSA*, 2022
- [6] M. Kontorovich and N. Lebedev, "On the one method of solution for some problems in diffraction theory and related problems," *J Exp Theor Phys*, 1938